Molecular Biology of the Cell
Vol. 17, 367–378, January 2006

An Uncleavable uPAR Mutant Allows Dissection of Signaling Pathways in uPA-dependent Cell Migration

Roberta Mazzieri,*† Silvia D'Alessio,*† Richard Kamgang Kenmoe,* Liliana Ossowski,‡ and Francesco Blasi,*§

*Department of Molecular Biology and Functional Genomics, Università Vita Salute San Raffaele and S. Raffaele Scientific Institute, 20132 Milan, Italy; §FIRC Institute of Molecular Oncology, 20116 Milan, Italy; and ‡Division of Hematology/Oncology, Department of Medicine, Mount Sinai School of Medicine, New York, NY 11029

Submitted July 15, 2005; Revised September 26, 2005; Accepted October 21, 2005
Monitoring Editor: Richard Assoian

Urokinase-type plasminogen activator (uPA) binding to uPAR induces migration, adhesion, and proliferation through multiple interactions with G proteins-coupled receptor FPRL1, integrins, or the epidermal growth factor (EGF) receptor (EGFR). At least two forms of uPAR are present on the cell surface: full-length and cleaved uPAR, each specifically interacting with one or more transmembrane proteins. The connection between these interactions and the effects on the signaling pathways activation is not clear. We have exploited an uPAR mutant (*hcr*, human cleavage resistant) to dissect the pathways involved in uPA-induced cell migration. This mutant is not cleaved by proteases, is glycosylphosphatidylinositol anchored, and binds uPA with a normal K_d. Both wild-type (wt) and *hcr*-uPAR are able to mediate uPA-induced migration, are constitutively associated with the EGFR, and associate with $\alpha3\beta1$ integrin upon uPA binding. However, they engage different pathways in response to uPA. wt-uPAR requires both integrins and FPRL1 to mediate uPA-induced migration, and association of wt-uPAR to $\alpha3\beta1$ results in uPAR cleavage and extracellular signal-regulated kinase (ERK) activation. On the contrary, *hcr*-uPAR does not activate ERK and does not engage FPRL1 or any other G protein-coupled receptor, but it activates an alternative pathway initiated by the formation of a triple complex (uPAR–$\alpha3\beta1$–EGFR) and resulting in the autotyrosine phosphorylation of EGFR.

INTRODUCTION

The serine protease urokinase-type plasminogen activator (uPA) and its high-affinity cell surface receptor (uPAR) play an important role in a number of physiological as well as pathological extracellular degradation processes, where cell migration is required, such as inflammatory responses and tumor invasion (Blasi and Carmeliet, 2002).

uPAR was first identified as a major player in the regulation of pericellular proteolysis by modulating and concentrating the uPA activity at the required sites of the cell surface (Blasi *et al*., 1987). However, new evidence revealed that uPA binding to uPAR also induces proteolysis-dependent and -independent intracellular signaling affecting cell adhesion, migration, and proliferation in a variety of cells (Chapman, 1997; Ossowski and Aguirre-Ghiso, 2000; Preissner *et al*., 2000; Blasi and Carmeliet, 2002; Kjøller, 2002).

uPAR is a heavily glycosylated glycosylphosphatidylinositol (GPI)-anchored protein (Ploug *et al*., 1991) formed by three cysteine-rich LY6-like extracellular domains (LU domains D1, D2, and D3) connected by short linker regions (Ploug and Ellis, 1994). The three consecutive three-finger domains of uPAR are organized in an almost circular manner and generate a deep internal cavity for the interaction with uPA. The receptor-binding domain of uPA is engaged in this central cavity, leaving the whole external surface available for other interactions (Llinas *et al*., 2005). Identified interactors include signaling molecules such as various integrins, the G protein-coupled receptor FPRL1, the epidermal growth factor (EGF) receptor (EGFR), the mannose-6-phosphate receptor, the family of low-density lipoproteins receptor-related proteins, p130, and others (Blasi and Carmeliet, 2002).

The linker region between D1 and D2 is a protease-sensitive region of uPAR that is cleaved by uPA producing a shorter form (D2D3), which no longer binds uPA. Other proteases cleave the linker region producing slightly different amino termini (Høyer-Hansen *et al*., 1992, 1997; Ragno *et al*., 1998; Sidenius *et al*., 2000; Koolwijk *et al*., 2001; Andolfo *et al*., 2002; Beaufort *et al*., 2004). The soluble form of D2D3 (s-D2D3) produced by uPA, in particular its AVTYSRSRY amino-terminal sequence, is a ligand for FPRL1 that induces chemotaxis (Resnati *et al*., 2002). Other receptors of the family of FPRL1 (FPR and FPRL2) have also been shown to respond to the same peptide sequence and to be desensitized by the uPAR

This article was published online ahead of print in *MBC in Press* (http://www.molbiolcell.org/cgi/doi/10.1091/mbc.E05–07–0635) on November 2, 2005.

† These authors contributed equally to this work.

Address correspondence to: Francesco Blasi (blasi.francesco@hsr.it).

Abbreviations used: EGF, epidermal growth factor; EGFR, epidermal growth factor receptor; ERK, extracellular signal-regulated kinase; *hcr*, human cleavage-resistant uPAR; ATF, amino-terminal fragment; GPI, glycosylphosphatidylinositol; fMLP, formyl-methyonyl-leucyl-proline; FPR, formyl-methyonyl-leucyl-proline receptor; IP, immunoprecipitation; JNK, c-Jun NH_2-terminal kinase; uPA, urokinase-type plasminogen activator; uPAR, urokinase-type plasminogen activator receptor.

chemotactic fragments (Furlan *et al*., 2004; Gargiulo *et al*., 2005; Selleri *et al*., 2005).

A second chemotactic region has been identified, in a charged residues-rich sequence in the major loop of the second domain of uPAR and shown to interact with $\alpha v\beta 3$ and $\alpha 5\beta 1$ integrins. Its chemotactic activity is exerted through an $\alpha v\beta 3$-dependent pathway involving Jak/Stat (Degryse *et al*., 2005). Both chemotactic regions of uPAR are located on the external surface of uPAR (Llinas *et al*., 2005). Additional uncharacterized uPAR sequences may also be involved in the uPAR/integrins interaction (Degryse *et al*., 2005). Counterpart regions in integrins that interact with uPAR has been previously recognized and comprise the entire upper loop of the W4 repeat in the b-propeller region of the α subunit of most integrins (Wei *et al*., 1996, 2001) and a $\beta 1$ peptide positioned nearby (Wei *et al*., 2005). Peptides that span these uPAR and integrin regions are able to prevent or dissociate uPAR from integrins (Wei *et al*., 1996, 2001, 2005; Degryse *et al*., 2005).

Another partner of uPAR is the EGFR. This transmembrane receptor coimmunoprecipitates with uPAR and can be constitutively activated by high levels of uPAR (Liu *et al*., 2002). In this case, the EGFR activation is $\alpha 5\beta 1$ integrin dependent, leads to the constitutive stimulation of the extracellular signal-regulated kinase (ERK) pathway and the down-regulation of the p38 mitogen-activating protein (MAP) kinase, determining cell proliferation in vivo. Moreover, uPA-induced migration may require ERK activation both in the presence and in the absence of EGFR (Degryse *et al*., 2001; Jo *et al*., 2005). In the absence of the EGFR, uPA induces pertussis-toxin sensitive (i.e., G protein-dependent) migration, whereas in the presence of EGFR the response is cell proliferation (Jo *et al*., 2005).

Thus, uPAR can act as an adhesion, migration, and proliferation receptor by shifting its association with its transmembrane partners. These activities, which have been found in cell culture, are functionally important in vivo because uPAR is required for the migration of cells in response to infections and inflammatory conditions, for the mobilization of hematopoietic stem cells, and for the growth and dissemination of tumors (Crowley *et al*., 1993; Min *et al*., 1996; May *et al*., 1998; Aguirre Ghiso *et al*., 1999; Gyetko *et al*., 2000; Aguirre-Ghiso *et al*., 2001; Selleri *et al*., 2005). Moreover, overexpression of uPAR by cancer and/or stromal cells is directly related to poor prognosis in a high percentage of human cancers (Danø *et al*., 1999; Sidenius and Blasi, 2003).

What is regulating uPAR association with the different transmembrane partners? At least three different forms of uPAR can be present on the cell surface: monomeric uPAR, dimerized uPAR, and cleaved uPAR (Høyer-Hansen *et al*., 1992; Cunningham *et al*., 2003). Each of these forms can have specific localization, transmembrane partners, and activity. In this article, we focused on uPA-induced cell migration and used a human uncleavable mutant of uPAR (*hcr*-uPAR) to shift the pool from cleaved to full length and differentiate between the various activities. We have determined the existence of individual pools of uPAR associated with specific transmembrane receptors, and the dynamic changes occurring upon binding of uPA. Moreover, the presence of unique activities associated with the *hcr*-mutant indicate that different forms and/or conformations of uPAR may select different signaling pathways.

MATERIALS AND METHODS

Reagents

Human two-chain uPA was obtained from Areta International (Varese, Italy), courtesy of Dr. M. Nolli. The amino-terminal fragment (ATF) of human uPA was a kind gift of J. Henkin (Abbott Laboratories, Abbott Park, IL). Production and purification of $D2D3_{88-274}$ was described previously (Fazioli *et al*., 1997). The murine monoclonal anti-human uPAR antibodies R2 and R3 (Rønne *et al*., 1991) and the rabbit polyclonal anti-human uPAR antibody were kindly provided by Drs. E. Rønne and G. Høyer-Hansen (Finsen Laboratory, Copenaghen, Denmark) and purified through a MAbTrap (GE Healthcare, Little Chalfont, Buckinghamshire, United Kingdom). The rabbit anti-human uPAR polyclonal serum has been described previously (Resnati *et al*., 1996). The MMK1 has been described previously (Klein *et al*., 1998). Irrelevant rabbit and mouse (MOPC-21) IgG, the synthetic chemotactic peptide formyl-methyonil-leucyl-proline (fMLP), the phosphorylated (p)-ERK inhibitor PD98059, and phosphatidylinositol-specific phospholipase C (PI-PLC) were purchased from Sigma-Aldrich (St. Louis, MO). Peptides $\alpha 325$ (PRHRHM-GAVFLLSQEAG) and s325 (HQLPGAHRGVEARFSML) were synthesized by PRIMM (Milan, Italy). Recombinant pertussis toxin (PTX) was a generous gift of Dr. M. G. Pizza (Chiron, Siena, Italy). The p-c-Jun NH_2-terminal kinase (JNK) inhibitor SP600125 was kindly provided by Prof. M. Del Rosso (University of Firenze, Florence, Italy). EGF was a generous gift of Dr. L. Beguinot (H. S. Raffaele, Milan, Italy). Tyrphostin AG1478, a p-EGFR inhibitor was from Calbiochem (San Diego, CA). FuGENE and *N*-glycosidase F were from Roche Diagnostics (Indianapolis, IN). The anti-FPRL1 polyclonal antibody (antibody N77) was generated as described previously (Furlan *et al*., 2004). Monoclonal anti-murine $\alpha 3$ and $\alpha 5$ integrins, polyclonal anti-EGFR, and monoclonal anti-total ERK2 antibodies were from Santa Cruz Biotechnology (Santa Cruz, CA). Monoclonal anti-mouse $\beta 1$ integrin antibody was from Chemicon International (Temecula, CA). Monoclonal anti-phosphotyrosine antibody was from Upstate Biotechnology (Lake Placid, NY), and a polyclonal antibody that specifically detects phosphorylated ERK1 and ERK2 was from Cell Signaling Technology (Beverly, MA). Horseradish peroxidase-conjugated antibodies specific for mouse IgG and rabbit IgG were from GE Healthcare.

Cell Lines and Culture Conditions

Murine fibroblast cell line LB6 were grown in DMEM (Invitrogen, Milan, Italy) supplemented with 10% fetal bovine serum (Sigma-Aldrich) and penicillin-streptomycin-glutamine (Invitrogen) at 37°C with 5% CO_2. LB6 clone 19 cells, expressing the wild-type human uPAR (Roldan *et al*., 1990), were grown in the same medium, supplemented with 0.5 mg/ml Geneticin (G418; Invitrogen). LB6 clones *hcr*16 and *hcr*15 were grown in the same medium, supplemented with 250 μg/ml hygromycin (Roche Diagnostics, Milan, Italy).

Generation of Stable Transfected hcr-uPAR Clones

The construction of the expression vector encoding for the human cleavage-resistant uPAR mutant (*hcr*-uPAR) was described previously (Liu *et al*., 2002). Proteases cleavage sites in the linker region between domain 1 and 2 were abolished by mutating R83K, Y87C, R89K, and R19K as described. LB6 cells were transfected with the *hcr*-uPAR construct using FuGENE under recommended conditions. Stably transfected cells were selected with hygromycin (100 μg/ml), and isolated clones were maintained in 100 μg/ml hygromycin. *hcr*-uPAR expression and cleavage resistance was determined by Western blot analysis on total cell extracts after deglycosylation as described below.

Cell Extracts, Western Blot Analysis, and Immunoprecipitation (IP)

Cell lysates were cleared by centrifugation at 15,000 rpm for 10 min at 4°C and quantitated by Bio-Rad protein assay (Bio-Rad, Hercules, CA). Equal amounts of each extract (50–80 μg) were then subjected to SDS-PAGE and electrotransferred to polyvinylidene difluoride membranes (Millipore, Billerica, MA) for direct immunoblotting. The membrane was incubated in blocking solution (Tris-buffered saline [TBS] containing 5% nonfat dried milk and 0.05% Tween 20) for 1 h at room temperature followed by 1 h of incubation with the indicated antibodies, three washes in TBS containing 0.05% Tween 20, and 1 h of incubation with donkey anti-rabbit horseradish-peroxidase-linked F(ab')2 fragment (1:5000; GE Healthcare). Proteins were detected using an enhanced chemiluminescence method according to the manufacturer's instructions (Pierce Chemical, Rockford, IL). For the detection of full-length and cleaved human uPAR, total cell extracts were first subjected to deglycosylation. Ten microliters of cell extracts containing 0.5% SDS and 2 mM dithiothreitol were incubated at 95°C for 3 min. Proteins were deglycosylated by addition of 20 μl of deglycosylation buffer (phosphate-buffered saline [PBS] containing 0.5% Triton X-100 and 15 mM EDTA) containing 1 U of *N*-glycosidase F and incubated at 37°C for 2 h. Deglycosylated samples were analyzed by SDS-PAGE under reducing conditions.

Where indicated, cells were pretreated with proteinases inhibitors (50 μM ilomastat, 80 μM E-64, 100 nM aprotinin, and 100 μmol/l amiloride) for 2 h and then treated with 10 nM uPA for the indicated times in the presence or in the absence of the same inhibitors.

For IP, total protein (0.5–1,5 mg) was precleared in PBS containing protein G agarose for 1 h at 4°C, and the supernatant was incubated with antibodies against murine EGFR or α3 integrin (1 μg/ml in PBS) overnight at 4°C. After washing with PBS, the immunoprecipitates were analyzed by Western blotting using the indicated antibodies.

Chemotaxis Assay

Migration of LB6 parental cell line and LB6 stable transfected clones was assessed by 48-well microchemotaxis chamber (Neuro Probe, Gaithersburg, MD). Chemoattractants (26 μl), at different concentrations in serum-free DMEM medium, were placed in the bottom compartment of the chamber, and a 200 μl of cell suspension (125,000 cells/ml) was added to the top compartment. The two compartments were separated by a fibronectin-coated (10 μg/ml) 8-μm-pore size polycarbonate filter (Neuro Probe) and incubated at 37°C in humidified air with 5% CO_2 for 5 h. The filter was removed, scraped, and stained with Diff-Quik (Dade Diagnostics, Aguada, Puerto Rico), and migrated cells were counted by light microscopy. Results expressed as the mean ± SD from triplicates samples are representative of at least three experiments. Migration in the absence of chemoattractant was set to 100%. Potential inhibitors of migrations (i.e., peptides, desensitizers, and pathway inhibitors) were preincubated with cells for 30 min at 37°C, and the assay was performed as described above.

Flow Cytometry

Cells (5×10^5) resuspended in 100 μl of staining buffer (PBS containing 2% fetal calf serum [FCS]) were incubated with the anti-human uPAR R2 antibody for 30 min on ice. Cells were washed with ice-cold staining buffer and resuspended in 100 μl of staining buffer containing Alexa 488-conjugated $F(ab')_2$ fragment of goat anti-mouse IgG (Invitrogen). After 30 min on ice, cells were washed with PBS, resuspended in 500 μl of PBS, and analyzed using a FACScan flow cytometer (BD Biosciences Italia, Milan, Italy). Dead cells were excluded from the analysis based on the forward and sideways light-scattering proprieties. Negative controls were provided by incubation with an irrelevant isotype-matched mouse antibody (MOPC-21), followed by staining with the same Alexa 488-conjugated secondary $F(ab')_2$ fragment of goat anti-mouse IgG.

When appropriate, human wild-type (wt)- and *hcr*-uPAR-expressing cells were incubated at a density of 10^6/ml in DMEM with 25 mM HEPES, pH 7.4, in the presence or in the absence of PI-PLC (5 U/ml) for 1 h at 37°C, as described previously (Ploug *et al*., 1991).

Ligand Binding Assay

Subconfluent cell monolayers, plated into 24-well plates the day before assay, were washed twice with PBS and incubated with increasing concentrations of ^{125}I-ATF (0.01–336 nM) (iodogen; Pierce Chemical), diluted in binding buffer (DMEM, 1% bovine serum albumin, and 20 mM HEPES) for 30 min at 4°C in the absence or in the presence of 100-fold excess of unlabeled uPA. After three washes with 1 ml of binding buffer, cells were lysed with 100 μl of NP-40 lysis buffer (150 mM NaCl, 1% NP-40, and 50 mM Tris-HCl, pH 8.0). Lysates were collected and counted in a gamma counter. Binding in the presence of 100-fold excess of unlabeled uPA was subtracted.

RESULTS

Properties of the Uncleavable hcr-uPAR

To investigate the role played by uPAR cleavage in uPA-mediated cell migration, a mutated form of the human uPAR (Liu *et al*., 2002) was used (Figure 1A). Four different amino acids substitutions were introduced to mutate all known cleavage sites located in the linker region between D1 and D2, thus generating a human cleavage-resistant (*hcr*) form of uPAR. The minimum chemotactically active region SRSRY (Fazioli *et al*., 1997) is mutated in the two arginines, although the essential (Trigwell *et al*., 2000) tyrosine is still intact. Murine LB6 cells that do not produce uPA and have a low level of endogenous murine receptor (Sidenius and Blasi, unpublished data) were stably transfected with *hcr*-uPAR, and two expressing clones were selected. A stably transfected and well characterized clone expressing wild-type human uPAR (LB6 cl19) was already available (Roldan *et al*., 1990; Riittinen *et al*., 1996).

Expression and cell surface localization of human wt-uPAR and *hcr*-uPAR were verified by cytofluorimetric analysis with the specific anti-uPAR antibody R2, using untreated or PI-PLC-treated cells. PI-PLC releases all GPI-anchored proteins from plasma membrane, including uPAR (Ploug *et al*., 1991). The level of uPAR expression evaluated by cytofluorimetry was very similar in both transfected clones and was reduced by PI-PLC treatment (data not shown).

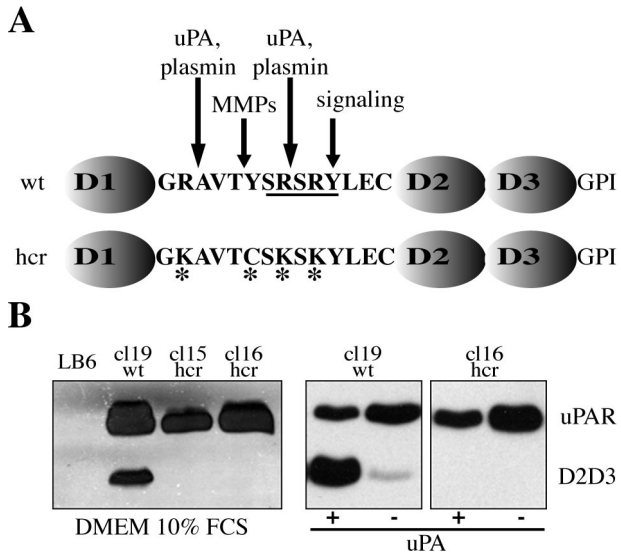

Figure 1. The human cleavage-resistant uPAR. (A) Schematic representation of wt-uPAR and *hcr*-uPAR. The amino acid sequence of the linker region between domains 1 and 2 is reported. The core sequence of the chemotactic epitope is underlined. Mutated residues in *hcr*-uPAR are marked by asterisk (*). Arrows indicate proteolytic cleavage sites and the signaling residue Tyr92. (B) Transfected clones showed a cell surface staining drastically reduced by PI-PLC treatment. Cells preincubated in the absence or in the presence of PI-PLC (1 U/ml) were stained with the monoclonal anti-uPAR antibody R2. Cell surface staining was verified by cytofluorimetric analysis. (C) Analysis of uPAR cleavage under culturing conditions (10% FCS, left) or after addition of exogenous human uPA (10 nM, right). Samples were deglycosylated and analyzed by Western blotting using a rabbit polyclonal anti-human uPAR antibody. Positions of intact (uPAR) and cleaved (D2D3) uPAR are indicated.

hcr-uPAR was also characterized for its ability to bind uPA using iodinated human ATF (the receptor binding, catalytically inactive fragment of uPA). Binding of ATF to both uPA receptors was saturable and specific because it was displaced by unlabeled human uPA. The three clones expressed comparable levels of surface receptors and bound uPA with about the same affinity (K_d of 1.2–2.4 nM) (data not shown).

We confirmed that *hcr*-uPAR was not cleavable by analyzing total cell extracts after deglycosylation and under reducing conditions by immunoblotting. LB6 cells stably transfected with the human wt-uPAR cDNA (cl19) and grown in the presence of 10% serum spontaneously generate a truncated form of uPAR that has the same molecular weight as the D2D3 form of uPAR (Figure 1B). The fraction of cleaved wt-uPAR varies between 10 and 50% of total uPAR depending on the culturing conditions (data not shown). Because LB6 cells produce no uPA, the cleavage of uPAR in the wt-uPAR cells in the absence of exogenous uPA must be due to a different protease. No cleaved uPAR was seen in the total cell extracts of *hcr*-uPAR cells (Figure 1B, left), nor was it cleaved upon addition of exogenous uPA (Figure 1B, right), a condition that led to an efficient cleavage of wt-uPAR.

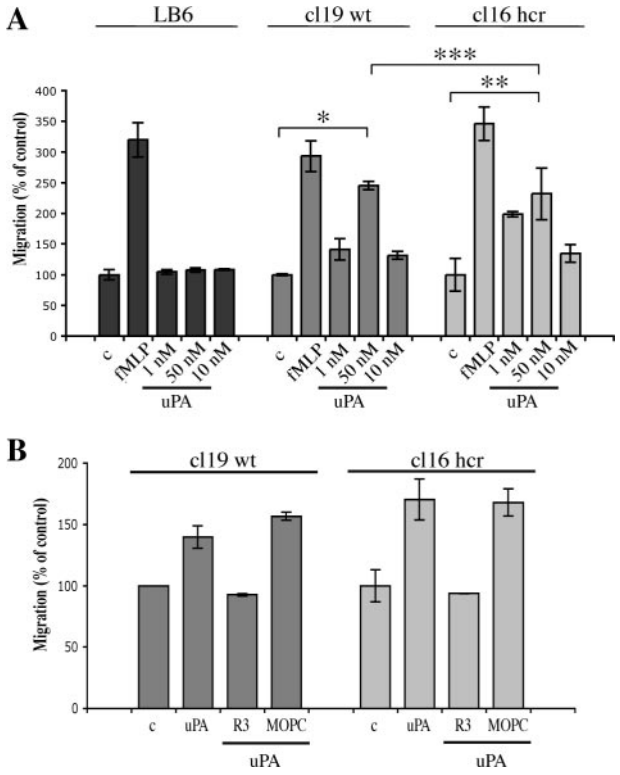

Figure 2. uPA-induced and uPAR-mediated migration of wt- and *hcr*-uPAR-expressing cells. (A) Chemotactic response of LB6 parental and transfected cells to human uPA. Cells migrated toward medium alone (control), fMLP (10^{-8} M), or increasing concentrations of human uPA (1, 10, and 50 nM). Random cell migration (c) of each cell line is referred to as 100% of migration. The data represent the average of nine independent experiments each in triplicates. *$p \leq 0.0014$, **$p \leq 0.0013$, ***$p \leq 0.87830$ (Student's *t* test). (B) Addition of R3 (monoclonal anti-uPAR antibody blocking uPA binding to uPAR) blocks uPA-induced migration of both wt- and *hcr*-uPAR-expressing cells. Cells migrated toward medium alone (c), uPA (10 nM), or uPA plus either R3 or irrelevant mouse IgGs (MOPC). Random cell migration (c) of each cell line is referred to as 100% of migration. Results are representative of three independent experiments.

Effects of the hcr Mutation on uPA-dependent and Unstimulated Cell Migration

Because it has been established that uPA/uPAR interactions are strictly species specific (Appella *et al*., 1987; Estreicher *et al*., 1989), murine uPAR is incapable of binding human uPA and thus LB6 parental cells do not display a chemotactic response to human uPA (Resnati *et al*., 1996) (Figure 2A). However, when stimulated with either an uPAR fragment, which contains the specific chemotactic epitope, 0.1 mM fMLP, which activates the same receptor as the uPAR chemotactic fragment or upon transfection with wild-type (wt) human uPAR and human uPA stimulation migration was induced, indicating that uPAR-mediated signaling is intact in these cells (Resnati *et al*., 1996; Fazioli *et al*., 1997). To test whether uPAR cleavage was necessary for cell migration, wt-uPAR and *hcr*-uPAR-expressing clones were analyzed for their ability to migrate on fibronectin in response to a human uPA gradient using a modified Boyden chamber assay. Incubation of wt-uPAR cells with human uPA induced, as expected, a dose-dependent chemotactic response, with a maximal effect at 10 nM. A similar chemotactic response was also observed in *hcr*-uPAR-expressing cells. No migration was induced by uPA in LB6 parental cells (Figure 2A). All cells equally responded to 0.1 mM fMLP, used as positive control.

To verify that the chemotactic response in both cell lines was because of a specific interaction between human uPA and human uPAR, cells were pretreated with either anti-uPAR monoclonal antibodies (R3) or with an equal amount of control monoclonal IgGs (MOPC-21). By recognizing an epitope localized on D1, R3 is able to block uPA binding to uPAR (Rønne *et al*., 1991). Addition of R3 completely blocked uPA-induced cell migration in both wt- and *hcr*-uPAR-expressing cells (Figure 2B). Together, these results show that both wt and *hcr* forms of uPAR mediate migration in response to uPA, suggesting that mutations in the linker region of uPAR that prevent its proteolytic cleavage do not block the ability of uPAR to mediate cell migration upon uPA stimulation.

Differential uPA/uPAR Signaling in wt- Versus hcr-uPAR-expressing Cells

The data presented in Figure 2A show that uPA-induced migration occurs both in the presence and in the absence of uPAR cleavage. However, the basal migration of the cells expressing the two forms of uPAR was different: the basal migration of both *hcr*-uPAR clones was similar to that of parental LB6 cells, whereas cl19, as expected, showed a substantially higher basal migration (data not shown). We therefore wondered whether wt-uPAR and *hcr*-uPAR use the same pathways to mediate cell migration.

Previous work established that uPAR interaction with integrins plays a role in uPA-induced migration (Wei *et al*., 1996). We first tested the involvement of $\alpha3\beta1$ and $\alpha5\beta1$ integrins, as they are well characterized transmembrane adaptor protein for uPAR (Wei *et al*., 2001). To test the interactions, we used a synthetic peptide, $\alpha325$, a 17-mer derived from the $\alpha3$ integrin sequence shown to block uPAR/$\alpha3\beta1$ and uPAR/$\alpha5\beta1$ interactions (Wei *et al*., 2001). uPAR/$\alpha3\beta1$ interaction was verified by immunoblotting analysis after immunoprecipitation with an anti-$\alpha3$ antibody in cells incubated with increasing concentrations of uPA. As shown in Figure 3A, incubation with uPA very strongly enhanced the interaction of both wt- and *hcr*-uPAR with the $\alpha3\beta1$ integrin, and the effect was dose dependent. The response of wt-uPAR to low concentration of uPA (1 nM) was appreciably stronger than that of *hcr*-uPAR. The uPAR/integrin interaction was inhibited in the presence of $\alpha325$ but not of a scrambled version of the peptide (s325). Moreover, only the full-length form of uPAR, and not D2D3, was found to associate with $\alpha3$-integrin. Similar expression levels of both $\alpha3\beta1$ and other integrins ($\alpha5\beta1$ and $\alpha v\beta3$) were observed in parental LB6 cells and in all transfected clones by immunoblotting analysis on total cell extracts (data not shown).

To investigate the role of uPAR/$\alpha3\beta1$ interaction on wt- and *hcr*-uPAR-mediated cell migration, chemotaxis experiments were carried out in the absence or in the presence of either $\alpha325$ or s325. Addition of $\alpha325$, but not of s325, strongly suppressed uPA chemotaxis, but it had no effect on FCS-induced chemotaxis in both wt-uPAR and *hcr*-uPAR cells (Figure 3B). Thus, both wt-uPAR and *hcr*-uPAR are interacting with the $\alpha3\beta1$ integrin, and this interaction is required to mediate uPA-induced cell migration.

We next tested whether cells expressing wt-uPAR or *hcr*-uPAR differed in the engagement of a second well-characterized transmembrane adaptor of uPAR, FPRL1 (Resnati *et al*., 2002). Because high concentrations (0.1 mM) of fMLP induce migration of LB6 cells (Figure 2A), these cells are

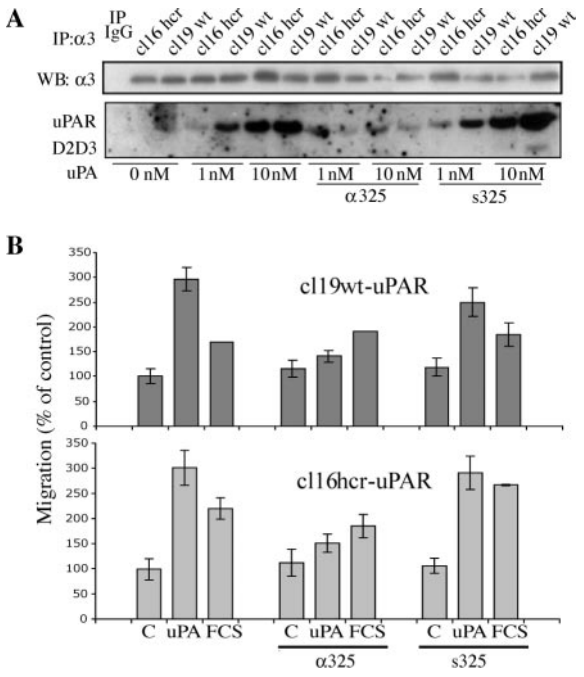

Figure 3. Integrins involvement in uPA-induced migration of wt- and *hcr*-uPAR-expressing cells. (A) uPAR/$\alpha3\beta1$ association is uPA dependent for both forms of uPAR, and addition of $\alpha325$ inhibits this association. Cells were pretreated for 20 min at 37°C with $\alpha325$ or s325 peptides (10 μM) and incubated for an additional hour with the indicated concentrations of uPA. $\alpha3$-Integrin was immunoprecipitated from total cell extracts using an anti-$\alpha3$ antibody. Immunoprecipitates were blotted for uPAR (bottom) and $\alpha3$ (top). (B) $\alpha325$ peptide specifically blocks uPA-induced migration in both wt- and *hcr*-uPAR-expressing cells. Cells were preincubated (20 min at 37°C) with $\alpha325$ or s325 peptides (10 μM), and their chemotactic responses were tested toward medium alone (c), uPA (10 nM), or FCS (2%). Random cell migration (c) of nonpretreated cells is referred to as 100% of migration. Results are representative of three independent experiments.

likely to express FPRL1. To verify the presence of FPRL1 (in the absence of an anti-murine FPRL1 antibody), we tested the chemotactic response of LB6 cells to increasing concentrations of the synthetic MMK1 peptide, a specific, high-affinity agonist for FPRL1 (Klein *et al*., 1998). MMK1 induced dose-dependent migration in all uPAR-expressing clones as well as in parental LB6 cells (data not shown). FPRL1 desensitization experiments by MMK1 pretreatment were then performed to verify FPRL1 involvement in uPA-induced migration. As shown in Figure 4A, MMK1 pretreatment completely suppressed uPA- and MMK1-, but not FCS-induced chemotaxis in wt-uPAR-expressing cells. However, desensitization of FPRL1 did not block uPA-induced migration in *hcr*-uPAR cells. We verified that all clones activated the FPRL1 pathway because they all were sensitive to sD2D3 that contains the amino-terminal chemotactic sequence, and to MMK1 desensitization (data not shown), as reported previously (Resnati *et al*., 2002).

Because uPA-induced migration in *hcr*-uPAR-expressing cells was not inhibited by MMK1-desensitization, we tested whether G-coupled receptors different from FPRL1 were involved in uPA-dependent *hcr*-uPAR-mediated migration using the ADP-ribosylating PTX. The inhibitory effect of PTX is an indication of the involvement of heterotrimeric $G_{i/o}$ proteins in the signaling pathway (Baggiolini *et al*., 1994; Neer, 1995). As expected, PTX efficiently blocked uPA and MMK1, but not FCS-induced migration in wt-uPAR-expressing cells (Figure 4B). On the contrary, no effect was seen on uPA-induced migration with *hcr*-uPAR-expressing cells, whereas the activity of MMK1 was still inhibited. This result indicates that a signaling pathway not involving a G protein-coupled receptor is activated by uPA in *hcr*-uPAR cells. We conclude that the mutations introduced in *hcr*-uPAR prevent the choice of the FPRL1 pathway.

To identify the alternative pathway engaged by *hcr*-uPAR, we explored another partner of uPAR: the EGF receptor (Liu *et al*., 2002; Jo *et al*., 2005). Both wt- and *hcr*-uPAR-expressing cells have similar levels of EGFR (Figure 5B). To probe the functional role of the EGFR, we tested the effect of the EGFR-specific inhibitor tyrphostin (AG1478) on uPA-dependent migration. As shown in Figure 5A, tyrphostin AG1478 completely blocked uPA-induced migration of *hcr*-uPAR cells but did not affect that of wt-uPAR-expressing cells. The effect was specific because AG1478 did not inhibit FCS-induced migration (which depends on the presence of a variety of serum factors). These results confirm that the two forms of uPAR engage two completely different pathways: wt (cleavable)-uPAR involves the FPRL1 pathway, whereas the cleavage-resistant uPAR involves the EGFR signaling pathway. We therefore tested for uPA-mediated EGFR tyrosine-phosphorylation in both wt-uPAR and *hcr*-uPAR cells. As shown in Figure 5B, uPA induced a strong phosphorylation of the EGFR only in the *hcr*-uPAR-expressing cells, which also have a higher basal level of p-EGFR. No EGFR phosphorylation was observed in wt-uPAR-expressing cells after addition of uPA. We can therefore conclude that the two forms of uPAR activate two different types of cell surface adaptor proteins. The lack of activation of EGFR by uPA in wt-uPAR LB6 cells may seem in contradiction with previous reports (Liu *et al*., 2002). However, the experiments reported in the present study are carried out in very different cells. LB6 are mouse cells, do not express uPA and have very low levels of endogenous murine uPAR (that does not bind human uPA), and have been transfected with human uPAR. Moreover, uPAR has been shown to be able to signal through different pathways in different cells (Jo *et al*., 2003, 2005).

The lack of G protein coupled receptor involvement and the activation of the EGFR in *hcr*-uPAR-mediated migration prompted an inquiry into the downstream signaling pathways of the wt- and *hcr*-uPAR cells. The involvement of two members of the MAP kinase family, ERK and JNK, was tested. wt- and *hcr*-uPAR-expressing cells were induced to migrate by uPA alone or uPA and either the mitogen-activated protein kinase kinase (MEK) inhibitor PD98059 or the JNK inhibitor SP600125. As shown in Figure 6A, the MEK inhibitor prevented both basal and uPA-induced migration of wt-uPAR-expressing cells but had no effect on *hcr*-uPAR-expressing cells. No inhibition was observed with the SP600125 JNK inhibitor (Figure 6B). We can, therefore, exclude an involvement of JNK and conclude that wt-uPAR and *hcr*-uPAR respond to uPA by activating different downstream signaling pathways. The inhibitory activity of PD98059 and SP600125 was verified by immunoblotting analysis after treatment of both wt- and *hcr*-uPAR cells with uPA. Both inhibitors efficiently reduced the basal levels of active ERK and JNK (Figure 6C). Moreover, PD98059 completely blocked the uPA-induced phosphorylation of ERK, which only occurs in the wt-uPAR-expressing cells (Figure 6C). Interestingly, Figure 6A shows that PD98059 also inhibited the basal migration of wt-uPAR-expressing cells, but not of *hcr*-uPAR-expressing cells. In fact, wt-uPAR cells have

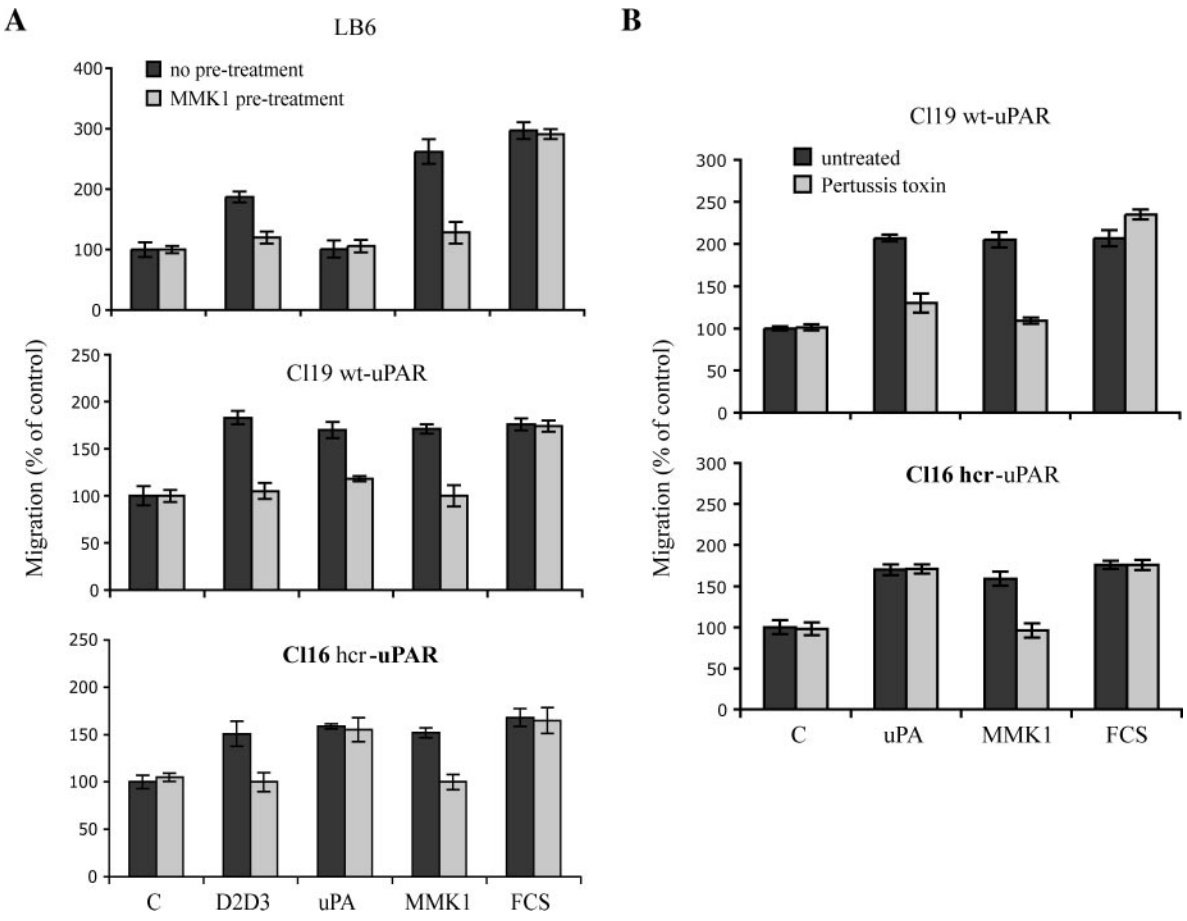

Figure 4. FPRL1 involvement in uPA-induced migration of wt-uPAR-expressing cells. (A) MMK1 specifically desensitizes uPA-induced chemotaxis in wt- but not *hcr*-uPAR-expressing cells. As controls, desensitization of FCS- and MMK1-induced migration (Resnati *et al*., 2002) is shown. For desensitization, cells were preincubated for 30 min at 37°C with MMK1 (10^{-6} M), and their chemotactic responses were tested toward medium alone (c), uPA (10 nM), MMK1 (10^{-6} M), or FCS (2%). Random cell migration (c) of nonpretreated cells is referred to as 100% of migration. Results are representative of three independent experiments. (B) Pertussis toxin specifically blocks uPA-induced migration in wt- but not *hcr*-uPAR-expressing cells. Cells were preincubated for 30 min at 37°C with pertussis toxin (100 ng/ml), and their chemotactic responses were tested toward medium alone (c), uPA (10 nM), MMK1 (10^{-6} M), or FCS (2%). Random cell migration (c) of nonpretreated cells is referred to as 100% of migration. Results are representative of three independent experiments.

a higher basal migration and a higher level of active ERK than hcr-uPAR cells (data not shown).

wt-uPAR and ERK Activation

wt-uPAR-expressing cells respond to uPA by engaging both integrins and FPRL1 (see above). To investigate which of these two transmembrane receptors was responsible for ERK activation in wt-uPAR cells, we performed a desensitization experiment with MMK1 and then induced the cells to migrate with uPA or sD2D3, which also is an agonist of FPRL1 (Resnati *et al*., 2002). As shown in Figure 7A, sD2D3 did not (or only marginally) activate ERK1/2 and the MMK1 pretreatment did not inhibit uPA-dependent ERK phosphorylation. Therefore, uPA-induced ERK phosphorylation was not achieved through FPRL1 activation. Moreover, addition of α325, but not of s325, to wt-uPAR cells inhibited uPA-induced phosphorylation of ERK (Figure 7B). The uPAR/integrins association is therefore necessary to activate ERK. These data suggest that in the case of wt-uPAR at least two pathways are activated upon uPA binding, one engaging FPRL1 and the other resulting in ERK activation. Both pathways are required for the induction of cell migration by uPA.

In addition, as shown in Figure 7C, integrins are involved in wt-uPAR cleavage because addition of α325, but not of s325, inhibited uPA-induced cleavage of uPAR. However, integrins are not required for the activation of FPRL1 (at least by sD2D3), because no inhibition of sD2D3-induced migration was seen in the presence of α325 (Figure 7D). Although soluble cleaved uPAR is known to activate FPRL1 (Resnati *et al*., 2002), no data are available about the ability of GPI-anchored uPAR to interact and/or activate FPRL1. Therefore, it remains to be established whether integrin-mediated uPAR cleavage activates FPRL1, ERK, or both pathways (see below).

The EGFR and hcr-uPAR Signaling

The next step was to analyze the role played by integrins in the EGFR pathway. As shown in Figure 8A, uPAR was coimmunoprecipitated by anti-EGFR antibodies in both wt- and *hcr*-uPAR cells. Only the full-length wild-type uPAR was found associated with the EGFR and addition of either uPA or α325 had no effect on both wt- and *hcr*-uPAR. Thus, the uPAR/EGFR association is integrin independent. However, the strong uPA-induced EGFR tyrosine phosphoryla-

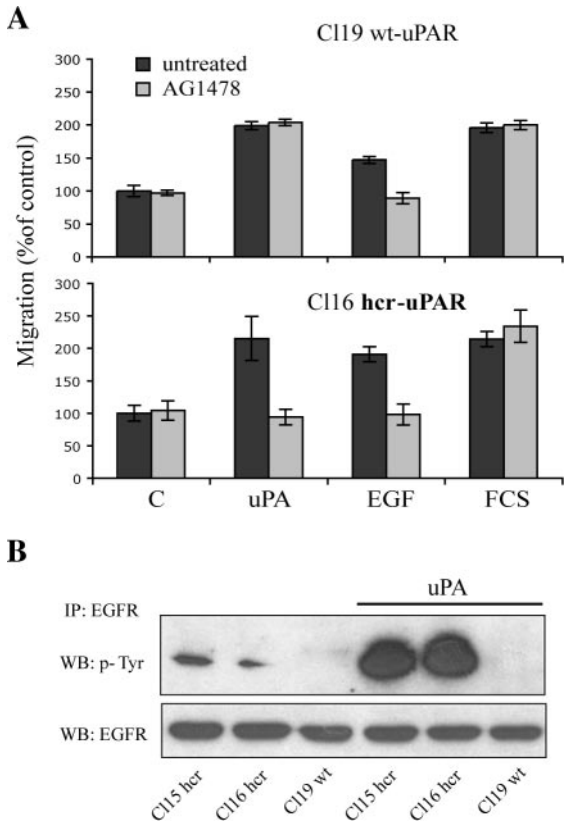

Figure 5. EGFR involvement in uPA-induced migration of *hcr*-uPAR-expressing cells. (A) The EGFR-inhibitor AG4178 specifically blocks uPA-induced migration in *hcr*- but not wt-uPAR-expressing cells. Cells were preincubated for 30 min at 37°C with AG4178 (50 nM), and their chemotactic responses were tested toward medium alone (c) or uPA (10 nM). Random cell migration (c) of nonpretreated cells is referred to as 100% of migration. Results are representative of three independent experiments. (B) uPA induces phosphorylation of EGFR in *hcr*- but not wt-uPAR-expressing cells. After 20-min stimulation with uPA, cell extracts were prepared and subjected to immunoprecipitation with an antibody against EGFR followed by immunoblot analysis to detect phosphorylated EGFR (p-Tyr) and total EGFR.

tion (as shown only in *hcr*-uPAR cells by immunoblotting with anti-p-tyrosine antibodies; Figure 5A) was completely inhibited by α325, thus showing the involvement of integrins in the activation of this pathway (Figure 8B).

We also investigated whether uPAR, $\alpha 3\beta 1$ integrin, and EGFR can associate into a ternary complex. We immunoprecipitated extracts from untreated and uPA-treated wt-uPAR and *hcr*-uPAR cells with anti α3 integrin antibodies and tested for the coprecipitation of uPAR and EGFR. As shown in Figure 8C (and previously in Figure 3A), uPAR association with the integrins was dependent on uPA in both cells. On the other hand, the association of the uPAR/$\alpha 3\beta 1$ complex with the EGFR occurred only in *hcr* cell extracts and was strongly increased by uPA.

Timing and Protease Dependence in uPA/uPAR Signaling

Last, to further analyze the relationship between signaling and cleavage, we compared the timing of activation of ERK and EGFR with that of uPAR cleavage upon addition of exogenous uPA. As shown in Figure 9A, wt-uPAR cleavage was visible already after 5–10 min and increased at least up to 60 min, at which time residual full-length uPAR was still present. The same time course was observed for ERK activation. To verify the cause–effect nature of this correlation, two different approaches were used. First, we added the catalytically inactive ATF. However, as shown in Figure 9A, addition of ATF resulted in abundant cleavage of uPAR and ERK activation, showing that ligand binding is sufficient to achieve uPAR cleavage by proteases other than uPA and that again cleavage is associated with ERK activation. Second, we added uPA in the presence of a cocktail of protease inhibitors (50 μM ilomastat, 80 μM E-64, 100 nM aprotinin, and 100 μmol/l amiloride). As shown in Figure 9B, the use of a cocktail of protease inhibitors supported the requirement of uPAR cleavage for uPA-dependent ERK activation, because inhibition of the cleavage in wt-uPAR-expressing cells correlated with the inhibition of uPA-mediated ERK phosphorylation. On the other hand, in *hcr*-uPAR-expressing cells, as shown in Figures 1C and 6C, there was no evidence of uPAR cleavage or of ERK activation; the EGFR phosphorylation started 20 min after uPA addition. Surprisingly, ATF did not induce EGFR phosphorylation in these cells (Figure 9A). However, these data correlate well with the migration data. In fact, although ATF efficiently induced migration of wt-uPAR cells, no migration was observed with *hcr*-uPAR-expressing cells (data not shown). No phosphorylation of EGFR at any time point and with any treatment was observed in wt-uPAR-expressing cells. Together, these data indicate that ERK phosphorylation requires uPAR cleavage, whereas EGFR activation correlates with the lack of uPAR cleavage.

DISCUSSION

The use of a mutated uPAR (*hcr*-uPAR) has allowed the dissection of pathways through which uPAR can stimulate cell migration in LB6 cells (Figure 10).

The data presented show that the two forms of uPAR engage two completely different pathways. Both forms of uPAR are constitutively associated with the EGFR. Upon uPA stimulation, an EGFR-free pool of wt-uPAR or wt-uPAR dissociating from the EGFR, associate with $\alpha 3\beta 1$. On the contrary, in *hcr*-uPAR cells a ternary $\alpha 3\beta 1$–uPAR–EGFR complex is formed upon uPA addition. Moreover, in wt-uPAR, association to integrins is required to cleave uPAR and to activate two distinct but necessary pathways: FPRL1 and ERK pathways. On the contrary, *hcr*-uPAR, which does not activate ERK and does not engage FPRL1 or any other G protein-coupled receptor (GPCR), activates an alternative pathways initiated by the phosphorylation of the EGFR.

We have previously demonstrated that a G protein-coupled receptor (FPRL1) of the family of the FPR receptors, connected to an heterotrimeric G_i protein, functions as a transmembrane adapter upon either uPA or ATF binding to uPAR and can directly interact with the cleaved soluble form of uPAR sD2D3 (Resnati *et al*., 2002; Furlan *et al*., 2004). FPRL1 mediates migration by recognizing a chemotactic epitope of uPAR, located between the first and second domain and characterized by the sequence AVTYSRSRY (Fazioli *et al*., 1997; Nguyen *et al*., 2000; Resnati *et al*., 2002). Through this interaction, a signaling pathway is activated that includes a src-like kinase and ERK, both required for migration (Resnati *et al*., 1996; Degryse *et al*., 1999; Webb *et al*., 2000). The chemotactic fragment can not only be generated by its ligand uPA (Høyer-Hansen *et al*., 1992, 1997) but also by other proteases such as plasmin, cathepsin G, matrix metalloproteases, and neutrophil elastase (Høyer-Hansen *et al*., 1997; Koolwijk *et al*., 2001; Andolfo *et al*., 2002; Beaufort

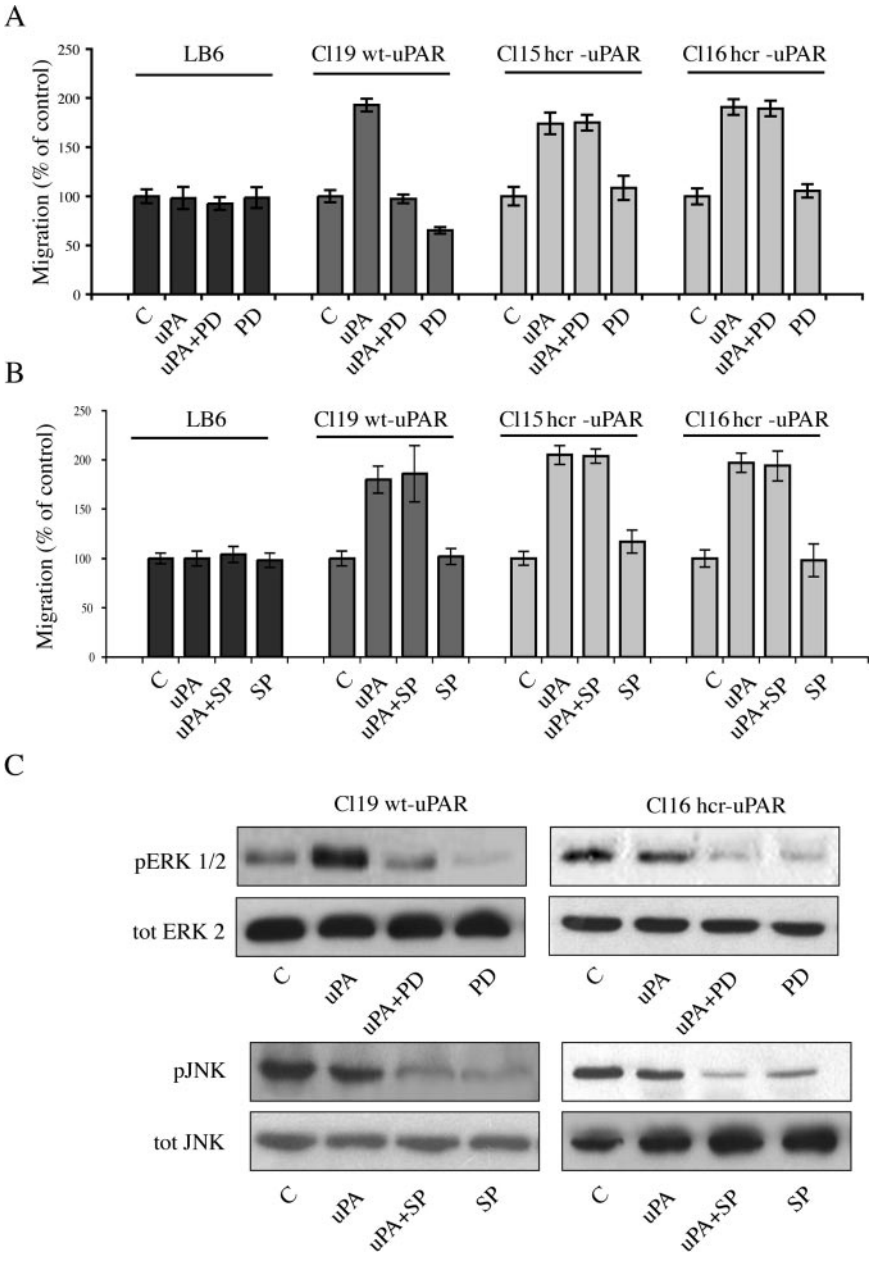

Figure 6. MAP kinases involvement in uPA-induced migration of wt- and *hcr*-uPAR-expressing cells. The ERK inhibitor PD98059 specifically blocks uPA-induced migration in wt- but not *hcr*-uPAR-expressing cells (A), whereas the JNK-inhibitor SP600125 has no effect (B). wt- and *hcr*-uPAR-expressing cells were induced to migrate toward an uPA gradient in the presence or in the absence of either PD98059 (50 μM) or SP600125 (50 μM). Random cell migration (c) of nonpretreated cells is referred to as 100% of migration. Results are representative of three independent experiments. (C) The inhibitory activity of PD98059 and SP600125 was verified by Western blotting after treatment of both wt- and *hcr*-uPAR cells with uPA. Both inhibitors efficiently reduced the basal levels of active ERK and JNK. Moreover, PD98059 completely blocked the uPA-induced phosphorylation of ERK which occurs only in the wt-uPAR cells.

et al., 2004). In fact, the present data also show that binding of the catalytically inactive ATF can still stimulate uPAR cleavage in the absence of uPA. FPRL1 activation seems to be caused by direct binding of the uPAR chemotactic epitope exposed by either ligand-induced conformational change, or proteolytic cleavage (Resnati *et al*., 1996, 2002).

hcr-uPAR is not cleaved by endogenous proteases nor by exogenous uPA (Figure 1C). Starting from its amino-terminal end, the first two mutations modify Arg83, a key residue for uPA cleavage, and Tyr87, cleavage site for chymotrypsin. These mutations lie outside the chemotactic region (which starts at residue 84) and are apart from the core sequence SRSRY starting at residue 88. The two other mutations lie within the core sequence SRSRY (Arg89 and Arg91). The first is not conserved in other species, but the peptide nevertheless still has chemotactic activity. Most importantly, residue Tyr92, an essential residue for signaling in this sequence (Trigwell *et al*., 2000) has not been mutated (Figure 1A). So far, no information is available on the role of Arg91. Because the amino acids substitutions are largely conservative, it was not unexpected that *hcr*-uPAR was normally expressed on the cell surface, could be released by PI-PLC, indicating GPI anchoring (Figure 1B), and could bind its ligand ATF with essentially a normal affinity. Despite being uncleavable by uPA, *hcr*-uPAR was still able to transduce the uPA chemotactic signal with essentially the same efficiency as wt-uPAR (Figure 2A). Moreover, both receptors are constitutively associated with the EGFR (Figure 8A) and are induced to associate to $\alpha 3\beta 1$ integrin upon uPA binding (Figure 3A). In spite of these similarities, however, the functional outcome of these interactions was different. Only in the *hcr*-uPAR cells uPA addition resulted in the formation of a ternary complex containing $\alpha 3\beta 1$, uPAR, and EGFR (Figure 8C) and in the activation of the EGFR (Figures 5B, 8B, and 9A). This suggests that the wt- and *hcr*-uPAR have a different conformation or that other unidentified proteins

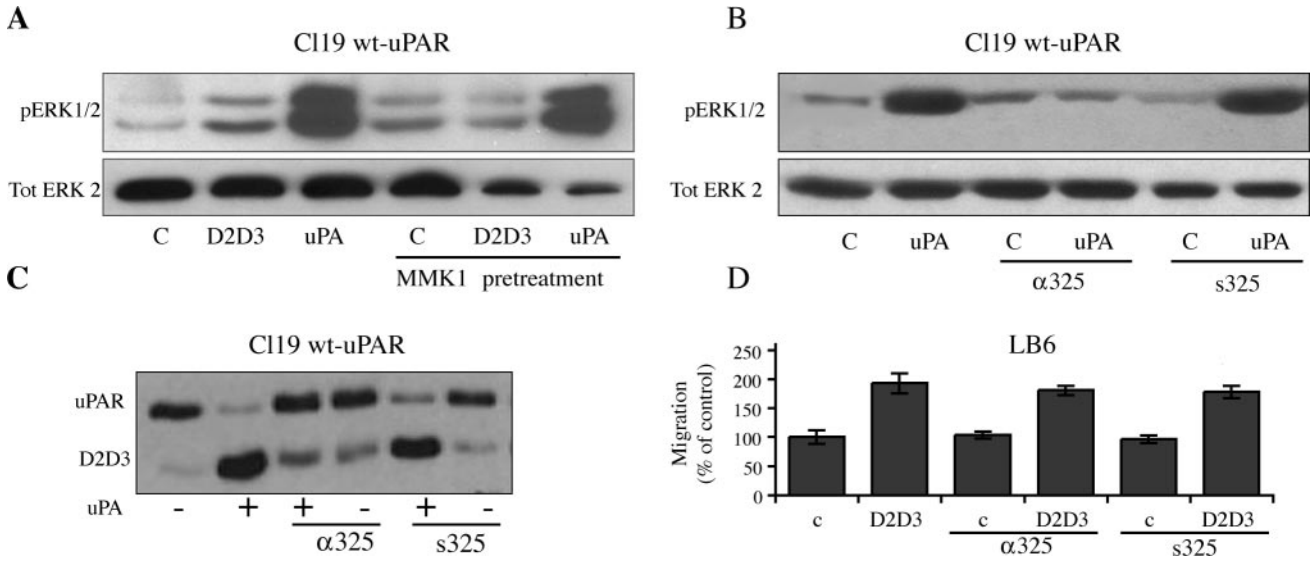

Figure 7. wt-uPAR/$\alpha 3\beta 1$ association, but not FPRL1 activation, is required to activate ERK. (A) MMK1 desensitization does not inhibit uPA-induced ERK phosphorylation, and stimulation with sD2D3 does not induced ERK phosphorylation. For desensitization, cells were preincubated for 30 min at 37°C with MMK1 (10^{-6} M) and treated with medium alone (c), uPA (10 nM), or sD2D3 (1 nM) for additional 40 min. Total cell extracts were analyzed by Western blot using an anti-phosphorylated ERK (p-ERK1/2) and an anti-total ERK (tot-ERK2) antibody. (B) $\alpha 325$ peptide specifically blocks uPA-induced phosphorylation of ERK. Cells were pretreated for 20 min at 37°C with $\alpha 325$ or s325 peptides (10 μM) and incubated for 40 min at 37°C in the absence (c) or in the presence of uPA (10 nM). Total cell extracts were analyzed by Western blot using an anti-phosphorylated ERK (p-ERK1/2) and an anti-total ERK (tot-ERK2). (C) $\alpha 325$ peptide specifically blocks uPA-mediated cleavage of uPAR. Cells were preincubated for 20 min at 37°C with $\alpha 325$ or s325 peptides (10 μM) and incubated for 40 min at 37°C in the absence (c) or in the presence of uPA (10 nM). Total cell extracts were deglycosylated and analyzed by Western blot using a rabbit polyclonal anti-uPAR antibody. Positions of intact (uPAR) and cleaved (D2D3) uPAR are indicated. (D) $\alpha 325$ peptide does not block SD2D3-induced migration of LB6 parental cells. Cells were preincubated for 20 min at 37°C with $\alpha 325$ or s325 peptides (10 μM), and their chemotactic responses were tested toward medium alone (c) or sD2D3 (1 nM). Random cell migration (c) of nonpretreated cells is referred to as 100% of migration. Results are representative of three independent experiments.

participate in the complexes assembled by the two forms of uPAR, causing differential activation of EGFR. Although understanding the molecular mechanisms behind the activation of the EGFR will require further investigations, the recent report of the crystal structure of uPAR and the modeling of its interaction with uPA (Llinas *et al.*, 2005) shows that the formation of a quadruple complex containing uPAR, uPA, $\alpha 3\beta 1$-integrin, and EGFR is possible and would not be prevented by uPA binding, because uPA binds to an internal cavity leaving the large external surface of the folded protein

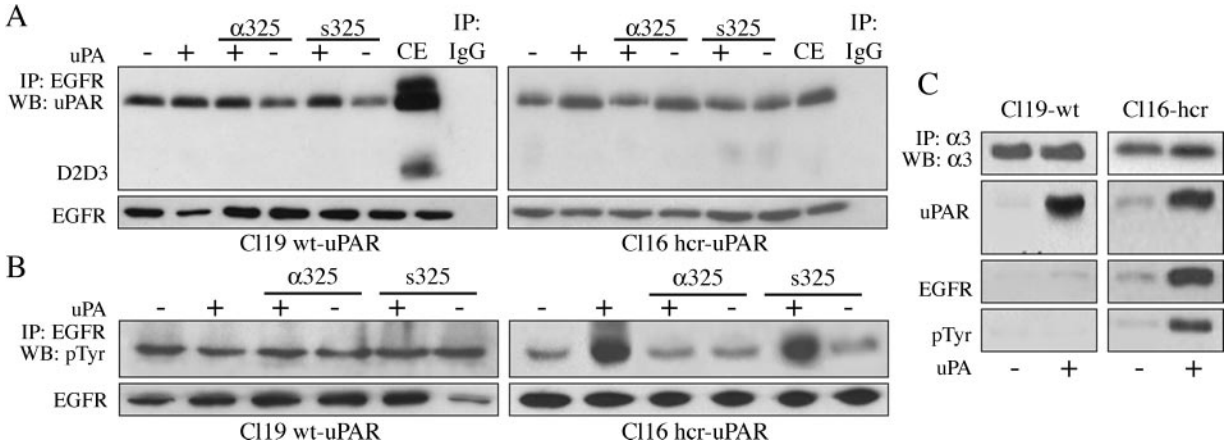

Figure 8. *hcr*-uPAR/$\alpha 3\beta 1$ association is required to activate EGFR. UPAR and EGFR are constitutively associated. UPA-induced phosphorylation of EGFR, only seen in *hcr*-uPAR cells, is specifically blocked by addition of $\alpha 325$. After a 20-min pretreatment with $\alpha 325$ or s325 peptides (10 μM), cells were stimulated with uPA (10 nM) for additional 20 min. EGFR was immunoprecipitated from total cell extracts with an anti-EGFR antibody and blotted for uPAR and EGFR (A) or phosphotyrosine and EGFR (B). CE is a control cell extract and a negative control used irrelevant immunoglobulin for immunoprecipitation (IP:IgG). (C) Extracts from wt- and *hcr*-uPAR cells, treated or not with 10 nM uPA, were immunoprecipitated with anti-$\alpha 3$ antibody, and the precipitate was immunoblotted with anti-uPAR, anti-EGFR, or anti-phosphotyrosine antibodies, as indicated.

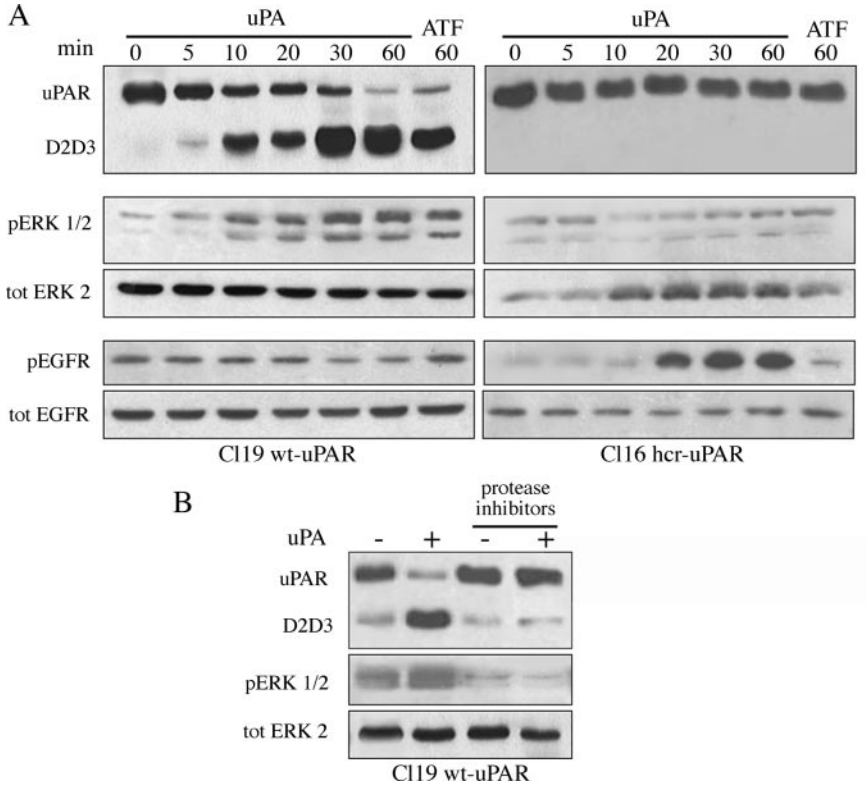

Figure 9. uPAR cleavage is required for uPA-dependent ERK activation in wt-uPAR cells. (A) Cells were treated with 10 nM uPA for the indicated times or with 5 nM ATF for 1 h. Total cell extracts were analyzed by Western blot using anti-phosphorylated ERK (p-ERK1/2) and EGFR (p-EGFR), and anti-total ERK (tot-ERK2) and EGFR (tot-EGFR) antibodies. For the detection of full-length and cleaved human uPAR, total cell extract were first subjected to deglycosylation as described in *Materials and Methods*. (B) wt-uPAR-expressing cells were preincubated with a cocktail of proteinase inhibitors (50 μM ilomastat, 80 μM E-64, 100 nM aprotinin, and 100 μmol/l amiloride) for 2 h and then treated with 10 nM uPA for 40 min at 37°C. Exogenous uPA failed to activate ERK in the presence of the inhibitors.

free to interact with $\alpha 3\beta 1$ and EGFR. Because in LB6 cells wt-uPAR does not associate with the EGFR and integrins in the same complex, we must hypothesize that the uPA-induced association between wt-uPAR and integrins may result in dissociation of wt-uPAR from the EGFR or in the recruitment to the integrin only of EGFR-free uPAR. In agreement with the immunoprecipitation data, although disruption of the uPAR/integrin interaction with peptide $\alpha 325$ specifically prevented migration activated through both forms of uPAR (Figure 3B), addition of an EGFR inhibitor only blocked *hcr*-uPAR-mediated migration (Figure 5A). As we further dissected the pathway engaged by the two forms of uPAR, we found that FPRL1 was only involved in wt-uPAR chemotaxis because the desensitization experiment with MMK1 peptide prevented the uPA-stimulated migration of wt-uPAR but not that of *hcr*-uPAR cells (Figure 4A). In agreement with these results, pertussis toxin only inhibited uPA-induced migration of wt-uPAR-expressing cells (Figure 4B). Together, the results with MMK1 and pertussis toxin not only confirm the involvement of FPRL1 in wt-uPAR-mediated migration but also rule out the involvement of any GPCR in *hcr*-uPAR migration.

The uPAR/EGFR interaction was shown to be involved in both cell migration (Jo *et al*., 2003) and tumor cell proliferation in vivo (Liu *et al*., 2002). It was also shown that uPAR-mediated activation of the EGFR requires an intact uPAR (Liu *et al*., 2002). A possible explanation of our results may indeed involve uPAR cleavage. The extent of cleavage of wt-uPAR by uPA or other proteinases may determine which of the two adaptor proteins (FPRL1 versus EGFR) will be engaged upon uPA binding to uPAR. However, activation of FPRL1 via GPI-D2D3 was not demonstrated yet. What we

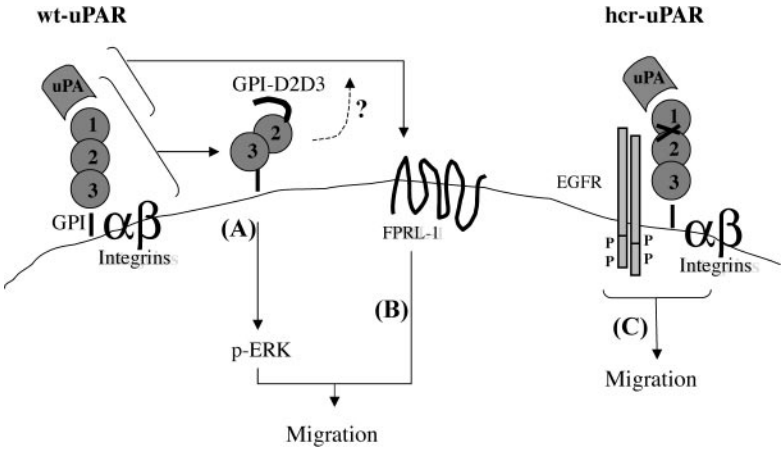

Figure 10. Schematic representation of uPA-induced pathways in wt- and *hcr*-uPAR cells. Scheme of the signaling pathways activated by wt-uPAR (left) and *hcr*-uPAR (right). (A) ERK activation via wt-uPAR upon uPA binding and association to $\alpha 3\beta 1$ and uPAR cleavage. (B) FPRL1 engagement via wt-uPAR upon uPA binding. (C) EGFR activation via *hcr*-uPAR upon uPA binding and association to integrins and EGFR.

demonstrated, and which further support the central role played by integrins, is that disruption of the uPAR/integrin interaction with peptide α325 prevents wt-uPAR cleavage mediated by uPA (Figure 7C). Moreover, in wt-uPAR-expressing cells, integrins (Figure 7B), but not FPRLI (Figure 7A), were also required for uPA-induced ERK activation, and the ERK1/2 inhibitor PD98059 totally prevented uPA-dependent chemotaxis of wt-uPAR, whereas it had no effect on *hcr*-uPAR (Figure 6A). uPA-induced ERK activation was also inhibited by a cocktail of protease inhibitors able to block uPAR cleavage (Figure 9B), thus suggesting the requirement of uPA-induced and integrin-mediated cleavage of uPAR to activate ERK. Inhibition of ERK also inhibited the basal migration of wt-uPAR-expressing cells (Figure 6A), which show a higher basal level of activated ERK and a higher random migration than parental LB6 cells or *hcr*-uPAR-expressing cells (data not shown). The cleavage of uPAR did not need to be carried out by uPA, because wt-uPAR LB6 cells cleave uPAR in the absence of exogenous uPA even though they do not express uPA (Figure 1C). Moreover, catalytically inactive ATF also stimulates uPAR cleavage in wt-uPAR cells (Figure 9A). This observation may be of particular interest in the context of tumor invasion, where several proteases, produced by tumor cells and/or surrounding host cells, are known to play an important role in tumor progression.

In conclusion our data show that uPAR can signal through several types of transmembrane receptors upon "activation" by several ligands and/or cleavage by different proteases. This allows a broad range of combinations determined both by the cell type induced to migrate and the surrounding environment. Understanding the specificity and selectivity of each combination will provide more direct and efficient tools for the control of uPAR-mediated migration under both physiological and pathological conditions such as tumor growth and tumor invasion.

ACKNOWLEDGMENTS

We are grateful to Drs. Anna Mondino and Laura Beguinot for reagents and helpful discussions. The work was supported by grants from the Italian Association for Cancer Research (AIRC 2005), the Cariplo Foundation and the EU (FP6 contracts 502935 and 503297) to F. B. and by U.S. Public Health Service Research Grant CA-40578 and the Samuel Waxman Cancer Research Foundation to L. O.

REFERENCES

Aguirre-Ghiso, J. A., Kovalski, K., and Ossowski, L. (1999). Tumor dormancy induced by downregulation of urokinase receptor in human carcinoma involves integrin and MAPK signaling. J. Cell Biol. *147*, 89–104.

Aguirre-Ghiso, J. A., Liu, D., Mignatti, A., Kovalski, K., and Ossowski, L. (2001). Urokinase receptor and fibronectin regulate the ERK (MAPK) to p38 (MAPK) activity ratios that determine carcinoma cell proliferation or dormancy in vivo. Mol. Biol. Cell *12*, 863–879.

Andolfo, A., English, W., Resnati, M., Murphy, G., Blasi, F., and Sidenius, N. (2002). Metalloproteases cleave of the urokinase-type plasminogen activator receptor leads to exposure of epitopes not present in the intact soluble receptor. Thromb. Haemost. *88*, 298–306.

Appella, E., Robinson, E. A., Ulrich, S. J., Stoppelli, M. P., Corti, A., Cassani, G., and Blasi, F. (1987). The receptor-binding sequence of urokinase. A biological function for the growth-factor module of proteases. J. Biol. Chem. *262*, 4437–4440.

Baggiolini, M., Dewald, B., and Moser, B. (1994). Interleukin 8 and related chemotactic cytokines-CXC and CC Chemokines. Adv. Immunol. *55*, 97–179.

Beaufort, N., Leduc, D., Rousselle, J. C., Magdolen, V., Luther, T., Namane, A., Chignard, M., and Pidard, D. (2004). Proteolytic regulation of the urokinase receptor/CD87 on monocytic cells by neutrophil elastase and cathepsin G. J. Immunol. *172*, 540–549.

Blasi, F., and Carmeliet, P. (2002). uPAR: a versatile signaling orchestrator. Nat. Rev. Mol. Cell. Biol. *3*, 932–943.

Blasi, F., Vassalli, J.-D., and Danø, K. (1987). Urokinase-type plasminogen activator: proenzyme, receptor and inhibitors. J. Cell Biol. *104*, 801–804.

Chapman, H. A. (1997). Plasminogen activators, integrins, and the coordinated regulation of cell adhesion and migration. Curr. Opin. Cell Biol. *9*, 714–724.

Crowley, C. W., Cohen, R. L., Lucas, B. K., Liu, G., Shuman, M. A., and Levinson, A. D. (1993). Prevention of metastasis by inhibition of the urokinase receptor. Proc. Natl. Acad. Sci. USA *90*, 5021–5025.

Cunningham, O., Andolfo, A. P., Santovito, A. L., Iuzzolino, L., Blasi, F., and Sidenius, N. (2003). Differential lipid raft partitioning of the urokinase receptor regulates its biological functions and is controlled by receptor dimerization. EMBO J. *22*, 5994–6003.

Danø, K., Romer, J., Nierlsen, B. S., Bjorn, S., Pyke, C., Rygaard, J., and Lund, L. R. (1999). Cancer Invasion and tissue remodeling-cooperation of protease systems and cell types. APMIS *107*, 120–127.

Degryse, B., Orlando, S., Resnati, M., Rabbani, S. A., and Blasi, F. (2001). Urokinase/urokinase receptor and vitronectin/$\alpha v\beta 3$ integrin induce chemotaxis and cytoskeleton reorganization through different signaling pathways. Oncogene *20*, 2032–2043.

Degryse, B., Resnati, M., Czekay, R.-P., Loskutoff, D., and Blasi, F. (2005). Domain 2 of the urokinase receptor contains an integrin-interacting epitope with intrinsic signaling activity: generation of a new integrin inhibitor. J. Biol. Chem. *280*, 24792–24803.

Degryse, B., Resnati, M., Rabbani, S. A., Villa, A., Fazioli, F., Blasi, F. (1999). Src-dependence and pertussis-toxin sensitivity of urokinase receptor-dependent chemotaxis, and cytoskeleton reorganization in rat smooth muscle cells via the urokinase receptor. Blood *94*, 649–662.

Estreicher, A., Wohlwend, A., Belin, D., Schleuning, W. D., and Vassalli, J.-D. (1989). Characterization of the cellular binding site for the urokinase-type plasminogen activator. J. Biol. Chem. *264*, 1180–1189.

Fazioli, F., Resnati, M., Sidenius, N., Higashimoto, Y., Appella, E., and Blasi, F. (1997). The urokinase-sensitive region of the urokinase receptor is responsible for its potent chemotactic activity. EMBO J. *16*, 7279–7286.

Furlan, F., Orlando, S., Laudanna, C., Resnati, M., Basso, V., Blasi, F., and Mondino, A. (2004). The soluble D2D3(88-274) fragment of the urokinase receptor inhibits monocyte migration and integrin-dependent cell adhesion. J. Cell Sci. *117*, 2909–2916.

Gargiulo, L., Longanesi-Cattani, I., Bifulco, K., Franco, P., Raiola, R., Campiglia, P., Grieco, P., Peluso, G., Stoppelli, M. P., and Carriero, M. V. (2005). Cross-talk between fMLP and vitronectin receptors triggered by urokinase receptor-derived SRSRY peptide. J. Biol. Chem. *280*, 25225–25232.

Gyetko, M. R., Sud, S., Kendall, T., Fuller, J. A., Newstead, M. W., and Standiford, T. J. (2000). Urokinase receptor-deficient mice have impaired neutrophil recruitment in response to pulmonary *Pseudomonas aeruginosa* infection. J. Immunol. *165*, 1513–1519.

Høyer-Hansen, G., Ploug, M., Behrendt, N., Rønne, E., and Danø, K. (1997). Cell surface acceleration of urokinase-catalyzed receptor cleavage. Eur. J. Biochem. *243*, 21–26.

Høyer-Hansen, G., Rønne, E., Solberg, H., Behrendt, N., Ploug, M., Lund, L. R., Ellis, V., and Danø, K. (1992). Urokinase plasminogen activator cleaves its cell surface receptor releasing the ligand-binding domain. J. Biol. Chem. *267*, 18224–18229.

Jo, M., Thomas, K. S., O'Donnell, D. M., and Gonias, S. L. (2003). Epidermal growth factor receptor-dependent and –independent cell signaling pathways originating from the urokinase receptor. J. Biol. Chem. *278*, 1642–1646.

Jo, M., Thomas, K. S., Marozkina, N., Amin, T. J., Silva, C. M., Parsons, S. J., and Gonias, S. L. (2005). Dynamic assembly of the urokinase-type plasminogen activator signaling receptor complex determines the mitogenic activity of urokinase-type plasminogen activator. J. Biol. Chem. *280*, 17449–17457.

Kjøller, L. (2002). The urokinase plasminogen activator receptor in the regulation of the actin cytoskeleton and cell motility. Biol. Chem. *383*, 5–19.

Klein, C., Paul, J. I., Sauve, K., Schmidt, M. M., Arcangeli, L., Ransom, J., Truehart, J., Manfredi, J. P., Broach, J. R., and Murphy, A. J. (1998). Identification of surrogate agonists for the human FPRL1 receptor by autocrine selection in yeast. Nat. Biotechnol. *16*, 1334–1337.

Koolwijk, P., Sidenius, N., Peters, E., Sier, C.F.M., Hanemaaijer, R., Blasi, F., and van Hinsbergh, V.W.M. (2001). Proteolysis of the urokinase-type plasminogen activator receptor by metalloprotease-12. Implication for angiogenesis in fibrin matrices. Blood *97*, 3123–3131.

Liu, D., Aguirre-Ghiso, J. A., Estrada, Y., and Ossowski, L. (2002). EGFR is a transducer of the urokinase receptor initiated signal that is required for in vivo growth of a human carcinoma. Cancer Cell *1*, 445–457.

Llinas, P., Le Du, M. H., Gardsvoll, H., Danø, K., Ploug, M., Gilquin, B., Stura, E. A., and Menez, A. (2005). Crystal structure of the human urokinase plasminogen activator receptor bound to an antagonist peptide. EMBO J. *24*, 1655–1663.

May, A. E., Kanse, S. M., Lund, L. R., Gisler, R. H., Imhof, B. A., and Preissner, K. T. (1998). Urokinase receptor (CD87) regulates leukocyte recruitment via beta 2 integrins in vivo. J. Exp. Med. *188*, 1029–1037.

Min, H. Y., Doyle, L. V., Vitt, C. R., Zandonella, C. L., Stratton-Thomas, J. R., Shuman, M. A., and Rosenberg, A. (1996). Urokinase receptor antagonists inhibit angiogenesis and primary tumor growth in syngeneic mice. Cancer Res. *56*, 2428–2433.

Neer, E. (1995). Heterotrimeric G proteins: organizers of transmembrane signals. Cell *80*, 249–257.

Nguyen, D. H., Webb, D. J., Catling, A. D., Song, Q., Dhakephalkar, A., Weber, M. J., Ravichandran, K. S., and Gonias, S. L. (2000). Urokinase-type plasminogen activator stimulates the Ras/Extracellular signal-regulated kinase (ERK) signaling pathway andMCF-7 cell migration by a mechanism that requires focal adhesion kinase, Src, and Shc. Rapid dissociation of GRB2/Sps-Shc complex is associated with the transient phosphorylation of ERK in urokinase-treated cells. J. Biol. Chem. *275*, 19382–19388.

Ossowski, L., and Aguirre Ghiso, J. A. (2000). Urokinase receptor and integrin partnership: coordination of signaling for cell adhesion, migration and growth. Curr. Opin. Cell Biol. *12*, 613–620.

Ploug, M., and Ellis, V. (1994). Structure-Function Relationship in the receptor for urokinase-type plasminogen activator. Comparison to other members of the Ly-6 family and snake venom a-neurotoxins. FEBS Lett. *349*, 163–168.

Ploug, M., Rønne, E., Behrendt, N., Jensen, A. L., Blasi, F., and Danø, K. (1991). Cellular receptor for urokinase plasminogen activator: carboxyl terminal processing and membrane anchoring. J. Biol. Chem. *266*, 1926–1933.

Preissner, K., Kanse, S. M., and May, A. E. (2000). Urokinase receptor: a molecular organizer in cellular communication. Curr. Opin. Cell Biol. *12*, 621–628.

Ragno, P., Montuori, N., Covelli, B., Høyer-Hansen, G., and Rossi, G. (1998). Differential expression of a truncated form of the urokinase-type plasminogen-activator receptor in normal and tumor thyroid cells. Cancer Res. *58*, 1315–1319.

Resnati, M., Guttinger, M., Valcamonica, S., Sidenius, N., Blasi, F., and Fazioli, F. (1996). Proteolytic cleavage of the urokinase receptor substitutes for the agonist-induced chemotactic effect. EMBO J *15*, 1572–1582.

Resnati, M., Pallavicini, I., Wang, Y. M., Oppenheim, J., Serhan, C. N., Romano, M., and Blasi, F. (2002). The fibrinolytic receptor for urokinase activates the G protein-coupled chemotactic receptor FPRL1/LXA4R. Proc. Natl. Acad. Sci. USA *99*, 1359–1364.

Riittinen, L., Limongi, P., Crippa, M. P., Conese, M., Hernandez-Marrero, L., Fazioli, F., and Blasi, F. (1996). Removal of domain D2 or D3 of the human urokinase receptor does not affect ligand affinity. FEBS Lett. *381*, 1–6.

Roldan, A. L., Cubellis, M. V., Masucci, M. T., Behrendt, N., Lund, L. R., Danø, K., and Blasi, F. (1990). Cloning and expression of the receptor for human urokinase plasminogen activator, a central molecule in cell-surface plasmin dependent proteolysis. EMBO J. *9*, 467–474.

Rønne, E., Behrendt, N., Ellis, V., Ploug, M., Danø, K., and Høyer-Hansen, G. (1991). Cell-induced potentiation of the plasminogen activation system is abolished by a monoclonal antibody that recognizes the NH2-terminal domain of the urokinase receptor. FEBS Lett. *288*, 233–236.

Selleri, C., *et al*. (2005). Involvement of the urokinase-type plasminogen activator receptor in hematopoietic stem cell mobilization. Blood *105*, 2198–2206.

Sidenius, N., Sier, C.F.M., and Blasi, F. (2000). Shedding and cleavage of the urokinase receptor (uPAR): identification and characterisation of uPAR fragments *in vitro* and *in vivo*. FEBS Lett. *475*, 52–56.

Sidenius, N., and Blasi, F. (2003). The urokinase plasminogen activator system in cancer: recent advances and implication for prognosis and therapy. Cancer Metastasis Rev. *22*, 205–222.

Trigwell, S., Wood, L., and Jones, P. (2000). Soluble urokinase receptor promotes cell adhesion and requires tyrosine-92 for activation of p56/59(hck). Biochem. Biophys. Res. Commun. *278*, 440–446.

Webb, D. J., Nguyen, D. H., and Gonias, S. L. (2000). Extracellular signal-regulated kinase functions in the urokinase receptor-dependent pathway by which neutralization of low density lipoprotein receptor-related protein promotes fibrosarcoma cell migration and Matrigel invasion. J. Cell Sci. *113*, 123–134.

Wei, Y., Czekay, R.-P., Robillard, L., Kugler, M. C., Zhang, F., Kim, K. K., Xiong, J.-P., Humphries, M. J., and Chapman, H. A. (2005). Regulation of $\alpha 5\beta 1$ integrin conformation and function by urokinase receptor binding. J. Cell Biol. *168*, 501–511.

Wei, Y., Eble, J. A., Wang, Z., Kreidberg, J. A., and Chapman, H. A. (2001). Urokinase receptor promotes $\beta 1$ integrin function through interactions with integrin $\alpha 5\beta 1$. Mol. Biol. Cell *12*, 2975–2986.

Wei, Y., Lukashev, M., Simon, D. I., Bodary, S. C., Rosenberg, S., Doyle, M. V., and Chapman, H. A. (1996). Regulation of integrin function by the urokinase receptor. Science *273*, 1551–1555.